3D and Multispectral Imaging for Subcutaneous Veins Detection

Vincent C. Paquit[1,2], Kenneth W. Tobin[1], Jeffery R. Price[1] and Fabrice Mériaudeau[2,*]

[1]*Oak Ridge National Laboratory, Oak Ridge, TN 37831, USA;*
[2]*Université de Bourgogne, Laboratoire Le2i, 71200 Le Ceusot, FRANCE*
[*] *fmeriau@u-bourgogne.fr*

Abstract: The first and perhaps most important phase of a surgical procedure is the insertion of an intravenous (IV) catheter. Currently, this is performed manually by trained personnel. In some visions of future operating rooms, however, this process is to be replaced by an automated system. Experiments to determine the best NIR wavelengths to optimize vein contrast for physiological differences such as skin tone and/or the presence of hair on the arm or wrist surface are presented. For illumination our system is composed of a mercury arc lamp coupled to a 10nm band-pass spectrometer. A structured lighting system is also coupled to our multispectral system in order to provide 3D information of the patient arm orientation. Images of each patient arm are captured under every possible combinations of illuminants and the optimal combination of wavelengths for a given subject to maximize vein contrast using linear discriminant analysis is determined.

© 2009 Optical Society of America

OCIS codes: (100.0100) Image processing, (110.0110) Imaging systems, (120.0120) Instrumentation, measurement, and metrology.

References and links

1. E. M. C. Hillman, "Experimental and theoretical investigations of near infrared tomographic imaging methods and clinical applications," Ph.D. thesis, Department of Medical Physics and Bioengineering - University College London (2002).
2. E. M. C. Hillman and A. Moore, "All-optical anatomical co-registration for molecular imaging of small animals using dynamic contrast," Nature Photonics **1**(9), 526–530 (2007).
3. H. D. Zeman, G. Lovhoiden, C. Vrancken, and R. K. Danish, "Prototype vein contrast enhancer," Optical Engineering **44**(8), 086,401 (2005).
4. V. C. Paquit, F. Meriaudeau, J. R. Price, and K. W. Tobin, "Simulation of skin reflectance images using 3D tissue modeling and multispectral Monte Carlo light propagation," in *30th Annual International Conference of the IEEE Engineering in Medicine and Biology Society, 2008. EMBS 2008*, pp. 447–450 (2008).
5. V. C. Paquit, J. R. Price, R. Seulin, F. Mériaudeau, R. H. Farahi, J. Kenneth W. Tobin, and T. L. Ferrell, "Near-infrared imaging and structured light ranging for automatic catheter insertion," Medical Imaging 2006: Visualization, Image-Guided Procedures, and Display **6141**(1), 61411T (pages 9) (2006).
6. V. C. Paquit, J. R. Price, F. Mériaudeau, J. Kenneth W. Tobin, and T. L. Ferrell, "Combining near-infrared illuminants to optimize venous imaging," Medical Imaging 2007: Visualization and Image-Guided Procedures **6509**(1), 65090H (pages 9) (2007).
7. R. Anderson and J. Parrish, "The Optics of Human Skin," Journal of Investigative Dermatology (1981).
8. Z. Zhang, "Flexible Camera Calibration by Viewing a Plane from Unknown Orientations," IEEE International Conference on Computer Vision **1**, 666 (1999).
9. Z. Pan, G. Healey, M. Prasad, and B. Tromberg, "Face Recognition in Hyperspectral Images," IEEE Transactions on Pattern Analysis and Machine Intelligence **25**(12), 1552–1560 (2003).

#107509 - $15.00 USD Received 12 Feb 2009; revised 13 May 2009; accepted 15 May 2009; published 23 Jun 2009

10. R. A. Jarvis, "A Perspective on Range Finding Techniques for Computer Vision," IEEE Transactions on Pattern Analysis and Machine Intelligence **5**(2), 122–139 (1983).
11. J. Forest, J. M. Teixidor, J. Salvi, and E. Cabruja, "A Proposal for Laser Scanners Sub-pixel Accuracy Peak Detector," in *Workshop on European Scientific and Industrial Collaboration*, pp. 525–532 (Mickolj (Hungria), 2003).
12. P. E. Bezier, *Emploi des machines à commande numérique* (Masson et Cie., 1970). Translated by Forrest, A. Robin and Pankhurst, Anne F. as Numerical Control – Mathematics and Applications, John Wiley and Sons, Ltd., London, 1972.
13. A. Efremov, V. Havran, and H.-P. Seidel, "Robust and numerically stable Bézier clipping method for ray tracing NURBS surfaces," in *SCCG '05: Proceedings of the 21st spring conference on Computer graphics*, pp. 127–135 (ACM, New York, NY, USA, 2005).
14. V. C. Paquit, F. Meriaudeau, J. R. Price, and K. W. Tobin, "Multispectral Imaging For Subcutaneous Structures Classification And Analysis," in *International Topical Meeting on Optical Sensing and Artificial Vision, OSAV'2008, Saint Petersburg, Russia* (2008).
15. H. J. Noordmans, R. de Roode, and R. Verdaasdonk, "Compact multi-spectral imaging system for dermatology and neurosurgery," in *Medical Imaging 2007: Physics of Medical Imaging*, J. Hsieh and M. J. Flynn, eds., vol. 6510, p. 65100I (SPIE, 2007).
16. K. Fukunaga, *Statistical Pattern Recognition* (Morgan Kaufmann, 1990).
17. C. Steger, "Extraction of curved lines from images," in *Proceedings of the 13th International Conference on Pattern Recognition*, vol. 2, pp. 251–255 vol.2 (1996).
18. J. Staal, M. Abramoff, M. Niemeijer, M. Viergever, and B. van Ginneken, "Ridge-based vessel segmentation in color images of the retina," IEEE Transactions on Medical Imaging **23**(4), 501–509 (2004).
19. J. Soares, J. Leandro, R. Cesar, H. Jelinek, and M. Cree, "Retinal vessel segmentation using the 2-D Gabor wavelet and supervised classification," IEEE Transactions on Medical Imaging **25**(9), 1214–1222 (2006).
20. V. C. Paquit, "Imagerie multispectrale et modélisation 3D pour l'estimation quantitative des vaisseaux sanguins sous cutanés," Ph.D. thesis, Université de Bourgogne, Le Creusot, France (2008).

1. Introduction

Biomedical imaging techniques based on wave propagation phenomena in biological tissues are commonly used to detect and treat diseases but are also used to image non-invasively organs and biological structures inside the body. Amongst them, optical tomography is a growing imaging technique offering the advantages to be non-invasive, experimentally simple, repeatable and inexpensive. Optical tomography uses light which offers at specific wavelengths a large variety of interaction phenomena, functions of physiological changes at cellular and subcellular levels, and allows retrieving information on biological systems. Over the last decade, publications in the field have reported promising results as well as really surprising images of human [1] or animal organs [2], letting us envision the capabilities of biomedical imaging using light. However, in this field only few researches investigate subcutaneous veins visualization and measurement. Using light propagation properties of tissues in the near infrared range of light, Zeman et al. [3] developed and commercialized, via Luminetx, a device to locate subcutaneous veins and back project their position on the imaged skin surface for catheter insertion assistance. The device named VeinViewer works well on patient with clear skin tone and low fat content which are ideal conditions for near IR propagation onto the tissues. However, performance can decrease significantly based on poorly understood relations to various physiological parameters. This technology also provides no estimation of the relative depth or diameter of vessels, which are key factors in selecting the optimal vein [4]. In preliminary research [5, 6] we have described experiments to determine the best near-infrared (NIR) wavelengths to optimize vein contrast for physiological differences such as skin tone and the presence of hair on the arm or wrist surface but we also noticed a correlation between the skin tone and the projection matrix used for classification as well as misclassification of some pixels due to reflection events and skin structure changes. Further investigations on light propagation in biological tissues [7] indicate that imaging the skin under visible to NIR illuminations will provide interesting reflectance spectrum variability that can be used to improve our classification method. In this paper we are presenting an optimization of our localization process by reducing the misclassification rate

#107509 - $15.00 USD Received 12 Feb 2009; revised 13 May 2009; accepted 15 May 2009; published 23 Jun 2009
(C) 2009 OSA

of pixels using different multispectral projection techniques, a broadband illumination source, and including the influence of the skin surface topography evaluation. The paper is structured as follows: after presenting our acquisition system and its calibration, computational methods and algorithms used for the classification process are introduced, followed by the obtained results. At last a conclusion and future work are discussed.

2. Experimental setup

Our acquisition system is composed of a visible to NIR sensitive CMOS video camera, a NIR line-generating laser module and a broadband illumination source (Hg arc lamp) associated with a monochromator for illumination wavelength selection. The equipment is controlled by a computer to synchronize illumination selection and image capture. In order to avoid UV radiation injuries to the skin, a high-pass filter at 495nm is inserted between the lamp and the monochromator. The spectral range of study is comprised between 495nm and 945nm by 10nm step, the upper limit being determined by the spectral sensitivity of the camera in the near infrared. A liquid gel light guide is connected on one hand to the output of the illumination source and on the other hand to a two inches wide collimating probe to maintain uniform illumination on the surface of the skin. Fig. 1 is a picture of the acquisition system.

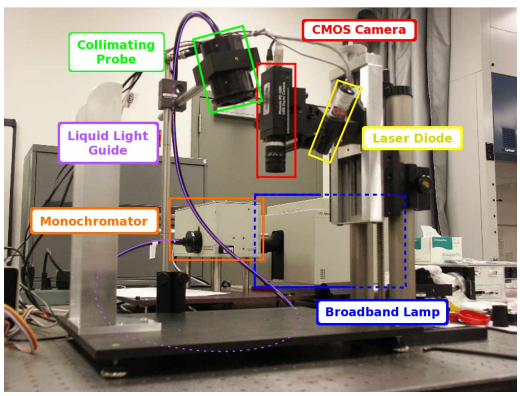

Fig. 1. Experimental setup

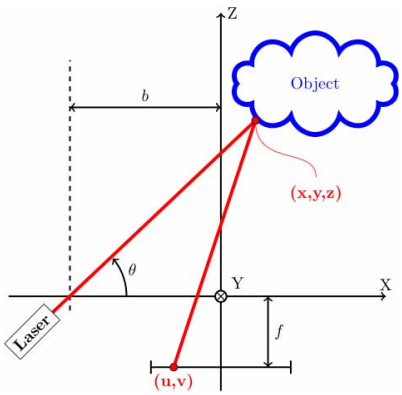

Fig. 2. Triangulation principle

The system calibration consists of three separate steps: (1) image distortion correction by retrieving the optical parameters of the camera [8], (2) reflectance image computation using black and white spectralons as references [9] and (3) parameterization of the triangulation geometry [10].

3. 3D reconstruction

Our 3D reconstruction process of the skin surface combines active optical triangulation for range data acquisition, and parametric surface modeling to store the 3D shape of the object. Active optical triangulation [10] combines a camera and a laser stripe line generator to recreate a basic geometric system. The camera is aligned along the Z axis and the laser line generator is positioned at a distance b from the camera with the angle θ relative to the X axis. Assuming that the considered laser point coordinates (x,y,z) in the 3D baseline has a projection (u,v) on the image plane, the similar triangles equations gives the mathematical relation between the measured quantities (u,v,θ) and the coordinates (x,y,z):

$$[x,y,z] = \frac{b}{f.\cot\theta - u}[u,v,f]. \tag{1}$$

#107509 - $15.00 USD Received 12 Feb 2009; revised 13 May 2009; accepted 15 May 2009; published 23 Jun 2009
(C) 2009 OSA

Experimental parameters i.e. the distance laser/optical axis b, the focal length f and the laser inclination θ are calculated during the system calibration and remain constant during the acquisition phase.

In a NIR image of the laser lines on the surface of the skin as on Fig. 3(a), the centerline of each line is firstly detected using a subpixel operator [11] which basically computes the zero crossing point of the first derivative of each stripe image row, see Fig. 3(b), and secondly triangulated using Equation 1. To simplify the three-dimensional surface modeling of the skin, the triangulated point clouds are associated with a Bézier surface [12]. At the same time the elevation map of the area of interest and the normal to the surface for each pixel using a specific ray tracing algorithm [13] are computed [14]. This data will be used later as a feature in the Linear Discriminant Analysis (LDA).

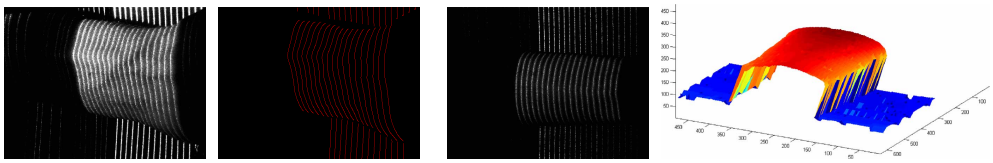

(a) (b) (c) (d)

Fig. 3. (a) image of the laser lines on the surface of the skin, (b) centerlines detected using a supbixel operator are in red, (c) Laser line on the forearm and (d) its 3D reconstruction.

4. Image Processing and Linear Discriminant Analysis

Multispectral imaging is commonly used to obtain reflectance measurements of an object in several spectral bands. As a result, each pixel of the image is expected to have specific intensity values over the light spectrum, corresponding to the so called spectral signature. Multipsectral imaging has found applications in the medical community, such as in dermatology or neurosurgery [15]. In our experiment, the skin is imaged from 495nm to 945nm by step of 10nm, giving a total of 46 images of the same scene. Different locations from hand to forehand were acquired for different patients. These aspects are currently being studied better location versus morphology/skin tone/bodymass index and are of special interest for young children where blood test are carried out on the top of the hand.

To analyze this 46-dimensional dataset a multispectral dimension reduction technique, which consists in projecting the initial dataset in a lower dimensional subspace where spectral information is more compact, and less correlated, was used. As stated before, our goal is to locate subcutaneous structures for various skin tones. This problem can be seen as a two class classification problem: vein/not-vein or a three class problem vein/skin/other. To reduce our dataset, two well-known linear dimension reduction techniques: Principal Component Analysis (PCA) [16] and Linear Discriminant Analysis (LDA) [16] were tried. Then, the resulting image corresponding to the projection of the initial data set onto the subspace spanned by the eigenvector of the first eigenvalue [14] was processed using the Stegers algorithm [17] to detect the veins as well as their respective width. The final goal being to select the optimal vein (size of the veins/catheter) in a short amount of time, Stegers algorithm was preferred to other algorithms as those used for retinal vessel segmentation [18, 19].

The surface orientation obtained after the triangulation and the normal of the surface is also added to the data set leading to a 47 input feature vectors. For the LDA, which requires a prior class identification in order to establish the projection matrix, the mask was automatically provided after processing the PCA image (see Fig. 4). Two labeling masks were used: (a) a two

#107509 - $15.00 USD Received 12 Feb 2009; revised 13 May 2009; accepted 15 May 2009; published 23 Jun 2009
(C) 2009 OSA

class mask vein / background, and (b) a three class mask vein / skin / background [20]

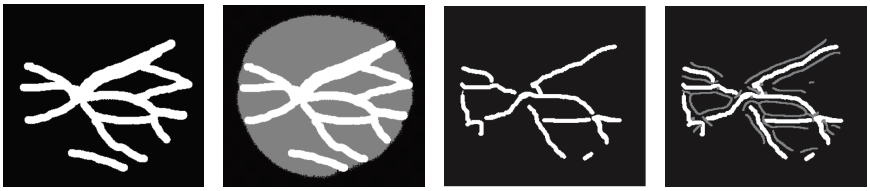

(a) (b) (c) (d)

Fig. 4. Example of the masks used for the LDA process. (a) Manually generated 2 class mask. (b)Aumatically (based on the PCA and Steger Algorithm) generated 2 class mask (c) Manually generated 3 class mask. (d)Aumatically (based on the PCA and Steger Algorithm) generated 3 class mask

Figure 5 is an example of some of the obtained results after projecting the data by LDA then extracting the veins. The first row corresponds to a two class problem where the mask for the class in manually defined by the operator and serves as a reference. The second row is for the two class problem with mask automatically generated from the PCA image. Third row corresponds to the 3 class problem with manually defined mask. Fourth row corresponds to the three class problem with mask automatically generated from the PCA image. This process was carried our over a panel of 20 patients having different skin tones and different body mass indexes. The results were similar showing that the 2 class problems with mask automatically generated and the input feature set including the 3D information provides results very close to those obtained with the manual mask. We also found out that the projection matrix for a specific skin tone can also be used for another patient of similar skin tone (based on the appearance compared to the Macbeth chart), however the opposite is not reliable [6]. Further experiment on a larger data set need to be run to see the influence of the body Mass index for similar skin tone patients. Moreover, based on our prior experiment on our restricted data set, it was not possible to isolate preponderant wavelength by looking at the eigenvalues obtained during the LDA. This point will be adressed when our database will be larger aiming at creating an "average" projection matrix which will be tested on similar skin tone (based on the appearance compared to the Macbeth chart) patients with various body mass index.

5. Conclusion

We showed in this paper a complete vision system providing multispectral as well as 3D information of the arm surface for automatic veins detection. The LDA projection of the multispectral images in the NIR and visible spectrum associated with 3D information of the arm topography lead to reliable results for automatic veins detection. However our long-term goal being to develop a fully-automated, vision-guided robotic system for needle insertion and catheterization, furthermore examination of the optimal wavelength combinations for different skin tone and/or presence of hair still need further investigation. We are also currently increasing our database to further validate the obtained results.

Acknowledgments

This manuscript has been authored by UT-Battelle, LLC, under contract DE-AC05-00OR22725 with the U. S. Department of Energy. Research sponsored by the Laboratory Directed Research and Development Program of Oak Ridge National Laboratory (ORNL), managed by UT-Battelle, LLC for the U. S. Department of Energy.

#107509 - $15.00 USD Received 12 Feb 2009; revised 13 May 2009; accepted 15 May 2009; published 23 Jun 2009
(C) 2009 OSA

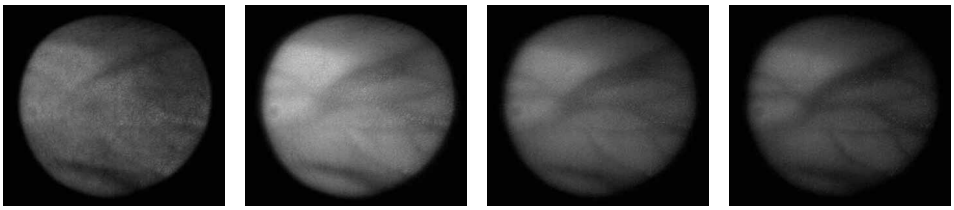

(a) Sample images of a dataset captured - from left to right - at 555nm, 655nm, 755nm, 855nm

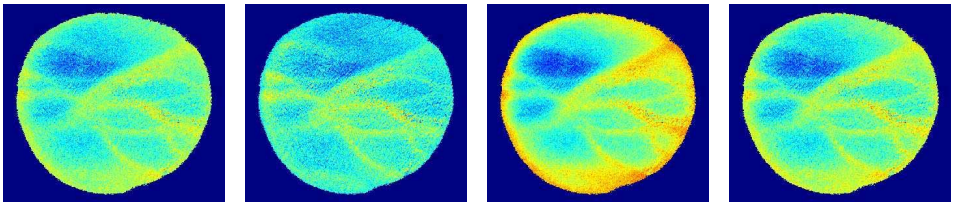

(b) LDA projections examples - from left to right - 2-class manual, 2-class auto, 3-class manual, 3-class auto

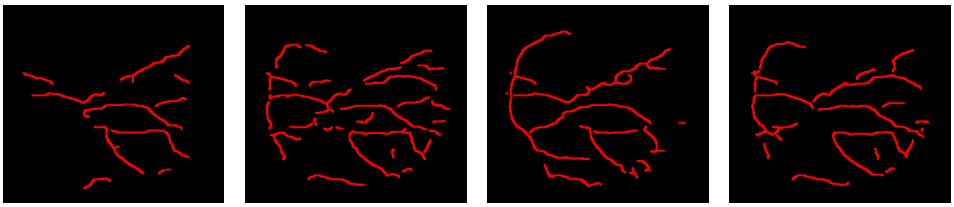

(c) Detection of the vascular centerlines on the LDA projection of NIR Data

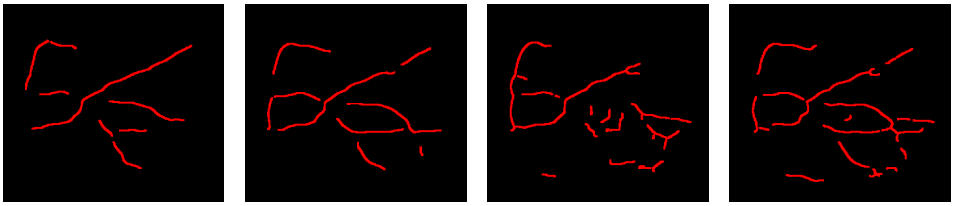

(d) Detection of the vascular centerlines on the LDA projection (NIR Data + 3D information)

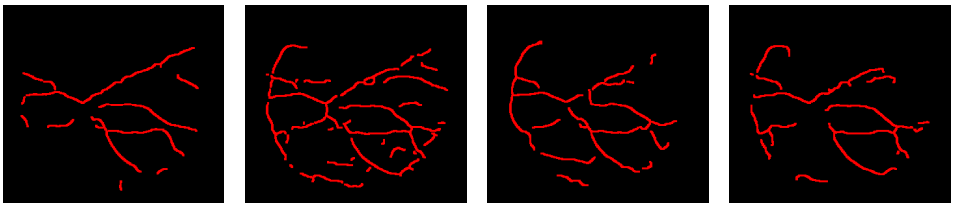

(e) Detection of the vascular centerlines on the LDA projection (NIR Data + Visible Data)

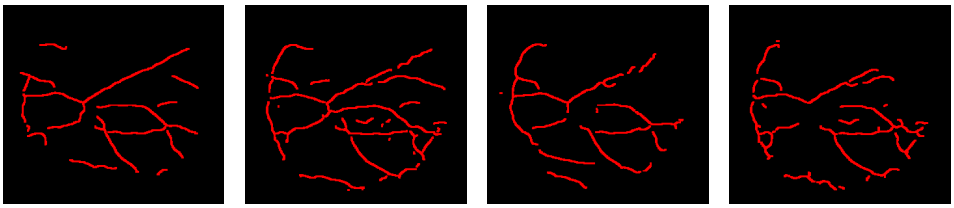

(f) Detection of the vascular centerlines on the LDA projection (NIR Data + Visible Data + 3D information)

Fig. 5. Comparison of the vascular centerline detection using Steger's algorithm for different input features and class masks: (first column) two class problem - vein/not vein - where the mask is manually defined; (second column) two class problem with mask automatically generated from the PCA image; (third column) three class problem - vein/skin/other -with mask manually defined; and (fourth column) three class problem with mask automatically generated from the PCA image.

#107509 - $15.00 USD Received 12 Feb 2009; revised 13 May 2009; accepted 15 May 2009; published 23 Jun 2009
(C) 2009 OSA